Antihydrogen Formation using Cold Plasmas

N. Madsen[*], M. Amoretti[†], C. Amsler[**], G. Bonomi[‡], A. Bouchta[‡], P. D. Bowe[*], C. Carraro[†], C. L. Cesar[§], M. Charlton[¶], M. Doser[‡], A. Fontana[††], M. C. Fujiwara[§§], R. Funakoshi[‡‡], P. Genova[††], J. S. Hangst[*], R. S. Hayano[‡‡], I. Johnson[**], L. V. Jørgensen[¶], A. Kellerbauer[‡], V. Lagomarsino[¶¶], R. Landua[‡], E. Lodi-Rizzini[***], M. Macri[†], G. Manuzio[¶¶], D. Mitchard[¶], P. Montagna[††], H. Pruys[**], C. Regenfus[**], A. Rotondi[††], G. Testera[†], A. Variola[†] and D. P. van der Werf[¶]

[*]*Department of Physics and Astronomy, University of Aarhus, DK-8000 Aarhus C, Denmark*
[†]*Istituto Nazionale di Fisica Nucleare, Sezione di Genova, I-16146 Genova, Italy*
[**]*Physik-Institut, Zürich University, CH-8057 Zürich, Switzerland*
[‡]*PH Department, CERN, Geneva, Switzerland*
[§]*Instituto de Fisica, Universidade Federal do Rio de Janeiro, Rio de Janeiro 21945-970, Brazil*
[¶]*Department of Physics, University of Wales Swansea, Swansea SA2 8PP, United Kingdom*
[‖]*Istituto Nazionale di Fisica Nucleare Sezione di Pavia, I-27100 Pavia, Italy*
[††]*Dipartimento di Fisica Nucleare e Teorica, Università di Pavia, I-27100 Pavia, Italy*
[‡‡]*Department of Physics, University of Tokyo, Tokyo 113-0033, Japan*
[§§]*Atomic Physics Laboratory, RIKEN, Saitama 351-0198, Japan*
[¶¶]*Dipartimento di Fisica di Genova, I-16146 Genova, Italy*
[***]*Dipartimento di Chimica e Fisica per l'Ingegneria e per i Materiali, I-25123 Brescia, Italy*

Abstract. Antihydrogen, the antimatter counterpart of the hydrogen atom, can be formed by mixing cold samples of antiprotons and positrons. In 2002 the ATHENA collaboration succeeded in the first production of cold antihydrogen. By observing and imaging the annihilation products of the neutral, non-confined, antihydrogen atoms annihilating on the walls of the trap we can observe the production in quasi-real-time and study the dynamics of the formation mechanism. The formation mechanism strongly influences the final state of the formed antihydrogen atoms, important for future spectroscopic comparison with hydrogen. This paper briefly summarizes the current understanding of the antihydrogen formation in ATHENA.

INTRODUCTION

Cold antihydrogen was produced by the ATHENA collaboration for the first time in 2002 [1]. The results were shortly thereafter confirmed by the ATRAP collaboration [2, 3]. The formation of cold antihydrogen, the antimatter counterpart of hydrogen, is the first step towards precision tests of fundamental symmetries in a pure antimatter system.

The ultimate goal, precision comparison of hydrogen and antihydrogen, may be based on precision measurements of the 1s-2s transition in a beam of cold hydrogen [4]. This method has been used to reach a record resolution of 1.8×10^{-14}. However, as antihydrogen may be difficult to produce in amounts large enough to make a beam, a more realistic goal will be to do spectroscopy on cold *trapped* antihydrogen as has also been

CP730, *Atomic Processes in Plasmas: 14th APS Topical Conference on Atomic Processes in Plasmas,*
edited by J. S. Cohen, S. Mazevet, and D. P. Kilcrease

done in hydrogen, though with lower precision [5]. This defines what we will term *useful* antihydrogen. Neutral traps have depths of order $\sim$1 K, and 1s-2s spectroscopy requires antihydrogen in the ground state. We thus need to, not only produce cold antihydrogen, but rather antihydrogen with a temperature of less then $\sim$1 K, and furthermore antihydrogen in its positronic ground state. A further interesting possibility would be to test the interaction of gravity with antimatter. Neutral antimatter makes this possible, although such measurements on antihydrogen would require temperatures at least as low as the mK regime in an optimistic estimate [6].

In order to be able to form *useful* antihydrogen understanding of the formation processes, and their dependence on temperature and the final states of the formed antiatoms, is necessary. This paper will describe the experimental approach of ATHENA towards these goals, as well as summarize the current status of the endeavor.

THE ATHENA APPARATUS

One ATHENA philosophy is to secure large amounts of cold antihydrogen in order to be in the best possible starting conditions for trapping the formed antiatoms. A distinctive feature of the ATHENA antihydrogen apparatus (Figure 1) is therefore its open and modular design. By avoiding a sealed vacuum, a powerful method of positron accumulation using buffer gas [7, 8] could be adopted while maintaining a vacuum of $\sim 10^{-14}$ mBar in which antiprotons survive for many hours. This makes the rapid and repeated introduction of 10's of millions of positrons possible. The open system allows for relatively easy introduction of laser light, and the possible extracting of antihydrogen atoms as a beam in the future.

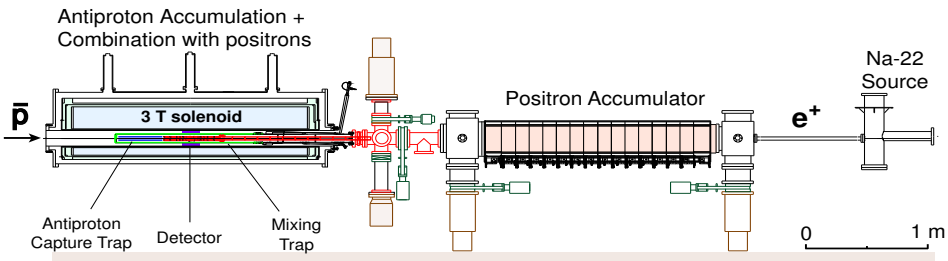

FIGURE 1. Overview of the ATHENA apparatus.

A high-granularity position sensitive detector [9] (Figure 2) was the key for unambiguous identification of the first production of antihydrogen atoms by detecting the annihilations of antiprotons and positrons occurring in spatial and temporal coincidence. Newly developed plasma diagnostic techniques [10, 11], allowed on-line monitoring of the conditions of the trapped positron plasma during its interaction with the antiprotons, as well as the possibility to heat the positron plasma non-destructively, providing an ability to rule out alternative (yet unlikely) interpretations of data, given e.g. in [2]. More details on the apparatus are given in Ref. [12].

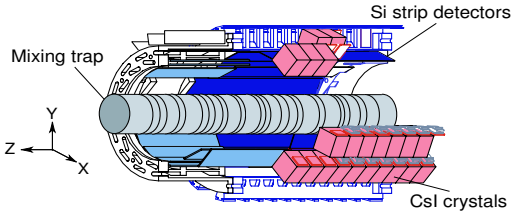

FIGURE 2. The ATHENA antihydrogen detector and the mixing trap shown in a cut-through drawing. The CsI crystals are cubes of $13\times17.5\times17$mm side lengths.

FIRST COLD ANTIHYDROGEN

Antiprotons for antihydrogen production are supplied by the CERN AD in spills of $2\text{-}3\times10^7$ antiprotons every 100 s. Those are degraded in a foil, and antiprotons with energy less than 5 keV are dynamically trapped in a Penning trap, where their radial motion is confined by a 3 T superconducting solenoid magnetic field. The antiprotons are then cooled by collisions with a batch of pre-loaded electrons. The electrons cool by emission of synchrotron radiation to near the ambient temperature of the trap of 15 K. A number of AD spills may be accumulated, and we usually accumulate 2-3 spills leaving us with $1\text{-}2\times10^4$ cold and trapped antiprotons for antihydrogen formation.

Positrons are obtained from a 40 mCi ^{22}Na source and immediately moderated by a frozen neon film. Trapping, cooling and accumulation are achieved using a nitrogen buffer gas, which provides the dissipative process for trapping the continuous flow of positrons. The method was pioneered by Surko and co-workers [7]. Around 150 million positrons are accumulated in the 0.14 T field every 5 min. after which they are transfered to the 3 T field with about 45% transfer efficiency. The transfer may be repeated and the positrons accumulated in the high field, in this way a record number of positrons of $>1.2\times10^9$ has been accumulated. In the high B-field Penning trap we can also apply a rotating electric field and compress the positron plasma [13]. A record density of $\sim1\times10^{11}$ cm^{-3} has been achieved in this way [14].

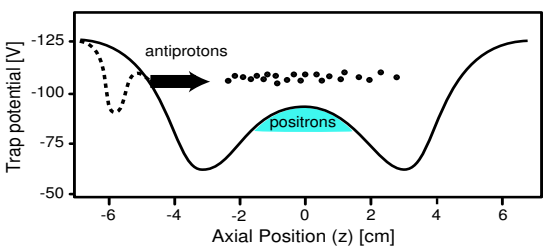

FIGURE 3. Nested trap configuration of the mixing trap for mixing positrons and antiprotons for antihydrogen formation. The potential on axis is given. The dashed curve indicates the potential before injection of the antiprotons.

Antihydrogen formation takes place in the so-called mixing trap, which is a double trap, where the positrons are housed in an inverted well at the center of the antiproton trap (Figure 3). This configuration is referred to as a nested trap [15]. Antihydrogen production is carried out by first loading the mixing trap with $\sim 7 \times 10^7$ positrons, which cool to the ambient temperature by the emission of synchrotron radiation, and then injecting about 10^4 antiprotons into the nested region where they interact through the Coulomb interaction with the positron plasma. The antiprotons are thus cooled by the positron plasma, and eventually, when the relative velocities are sufficiently low they may combine and form antihydrogen. This cooling process was first demonstrated by Gabrielse et al. [16], but with only $1/4$ million positrons. Figure 4 shows how the antiprotons loose energy when cooled by 70 million positrons [17]. When antiprotons are mixed with ambient temperature positrons we refer to the procedure as "cold" mixing. Alternatively the positron plasma may be heated by RF excitation to suppress antihydrogen formation [10]. Mixing with plasmas where the temperature has been increased by $\sim$3500 K we term "hot" mixing.

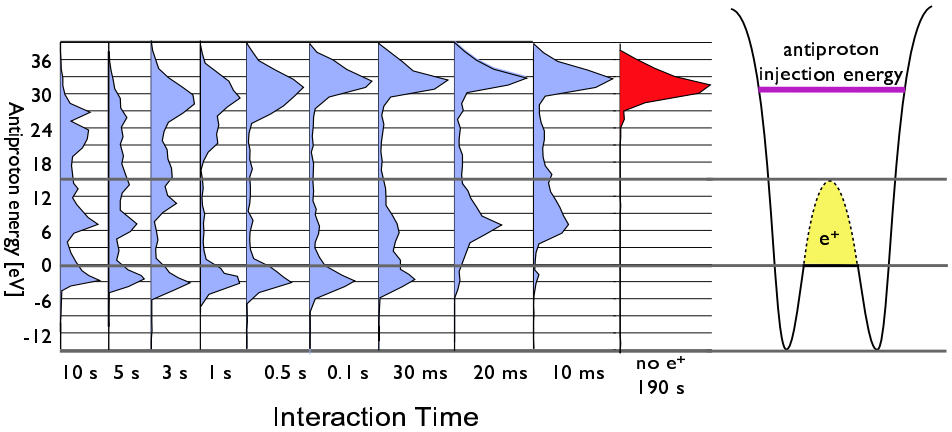

FIGURE 4. Cooling of antiprotons in the nested trap by interaction with the positrons. The energy distributions were measured by lowering the left trap wall and monitoring the number of antiprotons escaping as a function of the trap voltage by letting them annihilate on the degrader.

In a typical measurement we let the antiprotons interact with the positron plasma for about 180 s. before ejecting both species and restarting the cycle. The neutral antihydrogen atoms drift away from the formation region until they annihilate on the electrodes of the mixing trap. The antihydrogen detector can observe charged particle tracks using two layers of double-sided silicon microstrip detectors, and from these we can reconstruct the vertices of antiproton annihilations with a precision of $\sim$4 mm (1σ). The detector also observes the back-to-back 511 keV photons from the annihilation of positrons by highly segmented pure CsI crystals read out by avalance photodiodes [1, 9].

In our first observation we only accepted fully reconstructed pure antihydrogen events. To distinguish these we first demand a fully reconstructed antiproton annihilation vertex. Second we demand that the simultaneously hit crystals are isolated (i.e. no hits in the

neighboring crystals), have no charged tracks passing through, and that exactly two crystals are hit with the right energy photons. The photon energy window was set around 511±165 keV based on channel-by-channel in situ calibration using positron annihilation in the trap.

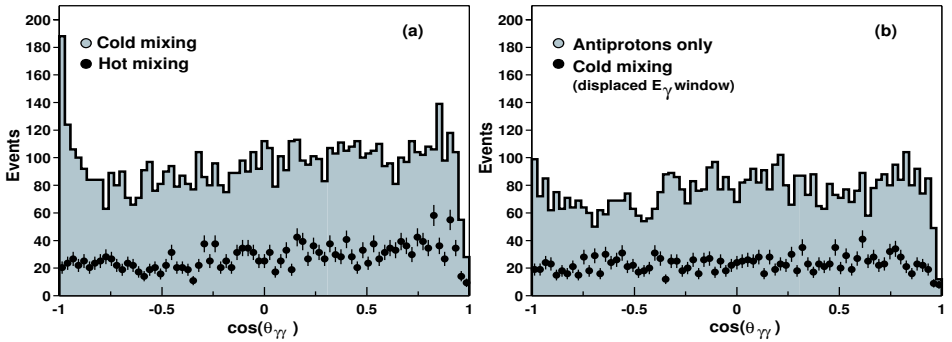

FIGURE 5. Cosine of the angle between two 511 keV photons, as seen from the antiproton annihilation vertex : (a) antiproton mixing with cold (ambient temperature) positrons (grey) and with positrons heated to ∼3500 K (circles). (b) without positrons and antiprotons annihilating on the wall (grey) and cold mixing, but analyzed with the photon energy window displaces to a region above 511 keV (circles) [1].

In Figure 5 we plot cosine of the angle $\theta_{\gamma\gamma}$ between the two hit crystals as seen from the antiproton annihilation vertex. This angle is called the opening angle. For real antihydrogen events a peak is expected at $\cos(\theta_{\gamma\gamma}) = -1$ which is what we observe. Also shown are a number of background situations in which no antihydrogen is produced, and indeed no peak at $\cos(\theta_{\gamma\gamma}) = -1$ is observed (for more discussion of background see Ref. [18]). The $\cos(\theta_{\gamma\gamma}) = -1$ peak in Figure 5 represents 131±22 antihydrogen atoms fully reconstructed.

HIGH RATE PRODUCTION

The cuts applied in the first observation reported above can conservatively be estimated to discard 99.7% of real antihydrogen events. The 131±22 events thus represents more than 50000 antihydrogen atoms produced. Further evidence of the real production being higher than the initial conservative estimate may be seen in Figure 6. The figure shows the cross-sectional (xy) distribution of all antiproton annihilations (no cuts applied) registered during cold and hot mixing respectively.

The distinct difference between Figure 6.a and Figure 6.b is the enhancement of annihilations at the trap wall during cold mixing. We recently published results where this enhancement, originating mainly from neutral antihydrogen drifting to and annihilating on the walls was fitted with a Monte-Carlo simulation of antihydrogen annihilating on the trap walls [19]. The fit gives a relative contribution of 69±5% of the annihilations stemming from the wall, when the hot mixing sample (Figure 6.b) is used as background. Careful analysis, including also fits to the radial distributions, as well as to the

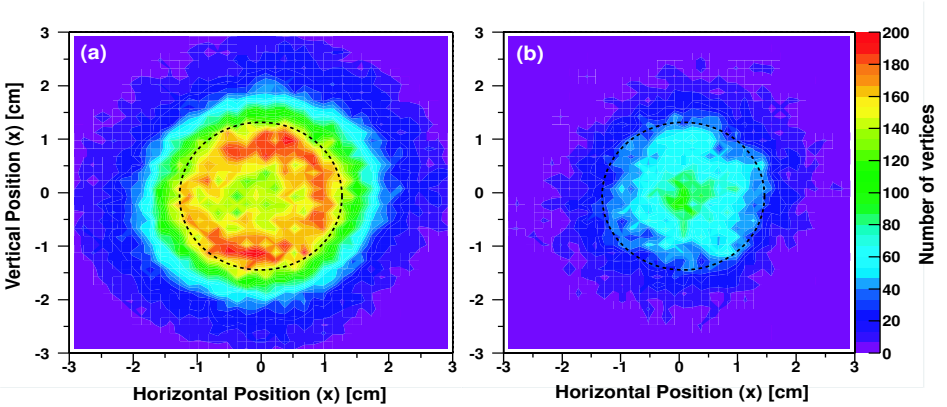

FIGURE 6. Cross sectional distribution (xy) of all antiproton annihilation vertices registered during cold (a) and hot (b) mixing. The black dashed circles mark the position of the trap walls. The cylindrical traps have a diameter of 25 mm.

opening angle distributions yielded a total estimated antihydrogen fraction in the sample of 65±5%. From the total number of accumulated mixing data in 2002 and 2003 we estimate that about 2.5 million antihydrogen atoms have been produced. This is equivalent to an efficiency of 15% of the mixed antiprotons. A few percent of the antiprotons annihilate on rest gas or positive ions trapped by the positron plasma, whereas the bulk of the antiprotons remain in the trap but in regions decoupled either axially (in the side wells of the nested-trap) or radially from the positron plasma [17].

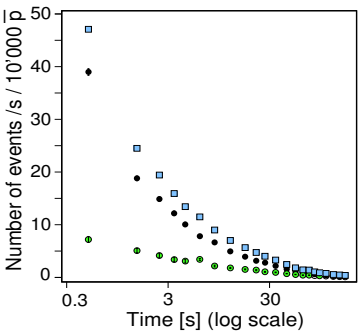

FIGURE 7. Number of vertices in the region $|z| < 4$ cm as a function of time after the start of cold mixing. Note the logarithmic time scale. Squares show the total number of vertices. The full circles shows the antihydrogen contribution as calculated from fits to the radial distribution. The grey circles show the background contribution.

Using analysis similar to the above to unravel the background and antihydrogen contribution to the annihilations at different points in time during the mixing we can

establish how the formation rate changes with time. Figure 7 shows a plot of the number of vertices as a function of time for vertices in a region given by $|z| < 4$ cm, where z is the axial position relative to the center of the positron cloud. This region was selected to avoid antiproton-only annihilations that dominate outside this region. Also shown is the fraction of antihydrogen and background at each point in time as extracted by radial fits to the vertex distributions. In this way we found that at early mixing times the antihydrogen production accounts for almost 90% of all detector triggers. Rates in excess of 200 Hz have been observed.

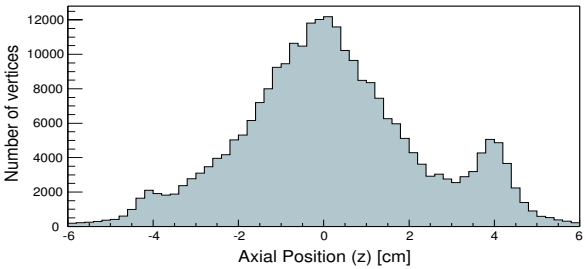

FIGURE 8. Axial distribution of antiproton annihilation vertices during cold mixing.

A powerful way to distinguish antihydrogen annihilations on the wall from antiproton-only annihilations arises from the observation that antiprotons annihilating on the walls annihilate in an azimuthally asymmetric way. Particles trapped in a Penning trap are, if nothing is done to actively prevent it, radially transported towards the walls of the trap were they will be lost. The rate of transport depends on a range of parameters of the system, however, we have observed using the antihydrogen detector that the losses are always localized, both axially and azimuthally [20]. Figure 8 shows a typical axial annihilation distribution from cold mixing. The left and the right peaks can be associated with antiproton-only losses as they are azimuthally localized as shown in Figure 9. The central structure is, as discussed earlier, composed of about 65% antihydrogen and 35% antiproton annihilations on rest gas or ions and is azimuthally symmetric. More details on annihilation imaging are given in Ref. [20].

TEMPERATURE DEPENDENCE

By applying a resonant RF field to excite the dipole mode of the positron plasma we can heat it [10]. Using this feature of our setup we have studied the temperature dependence of the formation of antihydrogen in our system [21]. Figure 10 shows the dependence of the peak trigger rate and the total number of triggers (backgrounds subtracted) as a function of the positron plasma temperature. We have used a no-heating temperature of 15 K, but this is not measured.

One expects two processes to be the main contributers to the formation in the present experimental conditions [22]. They are radiative formation, where a photon carries away

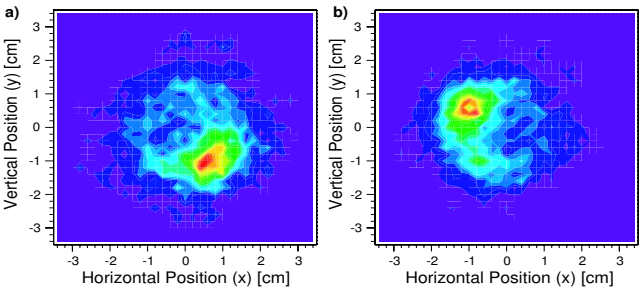

FIGURE 9. Cross sectional distributions of vertices from the two size peaks in Figure 8. (a) Left peak $-4.5 < z < -3.5$. (b) Right peak $3.5 < z < 4.5$.

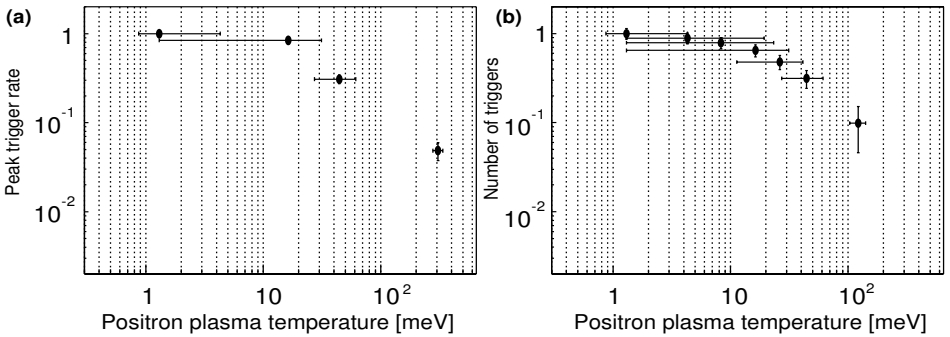

FIGURE 10. Formation dependence on positron temperature. (a) The peak detector trigger rate dependence. (b) The dependence of the total number of triggers in a mixing cycle.

the excess energy and momentum and 3-body formation where an additional positron carries it away [23, 24, 25]. The radiative process is expected to scale as $T^{-0.63}$ in zero magnetic field [25] and the 3-body process as $T^{-9/2}$ [26] where T is the positron temperature, which is expected to dominate as the antiprotons are much heavier than the positrons.

The measurements in Figure 10 shows that the formation only changes slowly with temperature for low temperatures and at around room temperature ($\sim$26 meV) the formation decreases as $\sim$T$^{-0.7}$. The expected strong rise in the formation at low temperatures where the 3-body process should dominate is thus absent. The persistence of formation at high temperature indicates at least some radiative contribution. However, the total measured rates are about a factor of 10 higher than a naive radiative calculation, neglecting the magnetic field, would suggest The behavior is thus not yet understood. A more detailed discussion of the results can be found in [21].

SUMMARY AND PERSPECTIVES

The ATHENA antihydrogen experiment and its recent experimental results were presented. ATHENA has, in 2002 and 2003 combined, produced more than 2.5 million cold antihydrogen atoms with formation rates in excess of 200 Hz. An overall efficiency amounting to $\sim$15% of mixed antiprotons forming antihydrogen has been observed.

The temperature dependence of the formation has been measured by RF heating of the positron plasma. The formation was observed to decrease only slightly with temperature for temperatures up to around 300 K and then decrease as $\sim T^{-0.7}$. The flattening at low temperature does not seem to agree with expectations that 3-body combination, scaling as $T^{-9/2}$, should dominate. The persistence of formation at room temperature indicates that radiative combination plays a role. More studies, both theoretical and experimental are needed to resolve these issues.

In 2004 ATHENA will pursue an experiment to laser-stimulate antihydrogen production in order to learn more on how to approach the ultimate goal of producing antihydrogen in its positronic ground state. The experiment is inspired by Ref. [27]. The ATHENA apparatus has been changed to allow access of a 50 W $^{13}C^{18}O_2$ laser which will couple the continuum and the $n = 11$ state in antihydrogen, where n is the principal quantum number. In this way we hope to circumvent the problems inherently involved in the spontaneous formation processes by directly controlling the final state of the formed antihydrogen. This will bring us closer to the goal of forming ground-state cold antihydrogen, and this experiment could therefore be an important mile stone on the way to precision spectroscopy of antihydrogen.

ACKNOWLEDGMENTS

We thank J. Rochet, S. Bricola, H. Higaki, G. Sabrero, and P. Chiggiato for their valuable contributions, and CERN's PS and AD crew for providing the excellent antiproton beam. This work was supported by FAPERJ (Brazil), INFN (Italy), MEXT (Japan), SNF (Switzerland), SNF (Denmark), EPSRC (UK).

REFERENCES

1. M. Amoretti et al., Nature **419**, 456 (2002)
2. G. Gabrielse et al., Phys. Rev. Lett. **89**, 213401 (2002)
3. G. Gabrielse et al., Phys. Rev. Lett. **89**, 233401 (2002)
4. M. Niering, *et al.*, Phys. Rev. Lett. **84**, 5496 (2000)
5. C. L. Cesar et al., Phys. Rev. Lett. **77**, 255 (1996)
6. G. Gabrielse, Hyp. Int. **44**, 349 (1988)
7. R.G. Greaves, M.D. Tinkle and C.M. Surko, Phys. Plasmas **1**, 1439 (1994)
8. L.V. Jørgensen et al., in: F. Anderegg, L. Schweikhard, C.F. Driscoll (Eds.), Nonneutral Physics, Vol. 4, American Institute of Physics, p. 35. (2002)
9. C. Regenfus, Nucl. Instr. and Meth. A **501**, 65 (2003)
10. M. Amoretti et al., Phys. Rev. Lett. **91**, 055001 (2003)
11. M. Amoretti et al., Phys. Plasmas **10**, 3056 (2003)
12. M. Amoretti et al.,Nucl. Inst. & Meth. A **518**, 679 (2004)

13. R. G. Greaves and C. M. Surko, Phys. Rev. Lett. 85, 1883 (2000)
14. M. Amoretti et al., submitted to Phys. Rev. Lett. (2004)
15. G. Gabrielse, S.L. Rolston, L. Haarsma, W. Kells, Phys. Lett. A **129**, 38 (1988)
16. G. Gabrielse et al., Phys. Lett. B **507**, 1 (2001)
17. M. Amoretti et al., accepted for Phys. Lett. B (2004)
18. M.C. Fujiwara et al., Nucl. Inst. & Meth. B **214**,11 (2004)
19. M. Amoretti et al., Phys. Lett. B **578**, 23 (2004)
20. M. C. Fujiwara et al., Phys. Rev. Lett. **92**, 065005 (2004)
21. M. Amoretti et al., Phys. Lett. B **583**, 59 (2004)
22. M.H. Holzscheiter and M. Charlton, Rep. Prog. Phys. **62**, 1 (1999)
23. H. A. Bethe and E.E. Salpeter, Quantum Mechanics of One- and Two-Electron Systems (Springer, Berlin, 1957).
24. P. Mansback and J. C. Keck, Phys. Rev. 181 (1969) 275.
25. J. Stevefelt, J. Boulmer and J-F. Delpech, Phys. Rev. A **12**, 1246 (1975)
26. M.E. Glinsky and T.M. O'Neil, Phys. Fluids B **3**, 1279 (1991)
27. A. Wolf, Hyp. Int. **76**, 189 (1993)